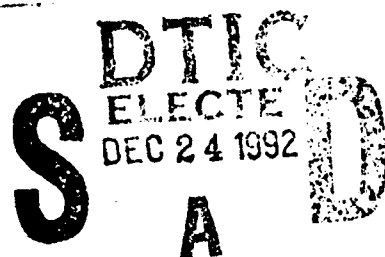


AD-A258 408



2

HEAT-TRANSFER MECHANISMS IN NAVY CLOTHING MATERIALS



NAVY CLOTHING AND TEXTILE RESEARCH FACILITY
NATICK, MASSACHUSETTS

00 70 28 1013
Approved for public release;
distribution unlimited.

TECHNICAL REPORT NO. 145

92-32759



Approved for public release; distribution unlimited.

Citation of trade names in this report does not constitute an official indorsement or approval of the use of such items.

Destroy this report when no longer needed. Do not return it to the originator.

UNCLASSIFIED

SECURITY CLASSIFICATION OF THIS PAGE (When Data Entered)

REPORT DOCUMENTATION PAGE		READ INSTRUCTIONS BEFORE COMPLETING FORM
1. REPORT NUMBER 145	2. GOVT ACCESSION NO.	3. RECIPIENT'S CATALOG NUMBER
4. TITLE (and Subtitle) HEAT TRANSFER MECHANISMS IN NAVY CLOTHING MATERIALS		5. TYPE OF REPORT & PERIOD COVERED Interim; 1979-1980
		6. PERFORMING ORG. REPORT NUMBER
7. AUTHOR(s) Norman F. Audet		8. CONTRACT OR GRANT NUMBER(s)
9. PERFORMING ORGANIZATION NAME AND ADDRESS Navy Clothing & Textile Research Facility 21 Strathmore Road Natick, MA 01760		10. PROGRAM ELEMENT, PROJECT, TASK AREA & WORK UNIT NUMBERS 62758N; 58523; 091; 523-003-57
11. CONTROLLING OFFICE NAME AND ADDRESS Same as 9.		12. REPORT DATE December 1982
		13. NUMBER OF PAGES 32
14. MONITORING AGENCY NAME & ADDRESS (if different from Controlling Office)		15. SECURITY CLASS. (of this report) Unclassified
		15a. DECLASSIFICATION/DOWNGRADING SCHEDULE
16. DISTRIBUTION STATEMENT (of this Report) Approved for public release; distribution unlimited.		
17. DISTRIBUTION STATEMENT (of the abstract entered in Block 20, if different from Report) Same as 16.		
18. SUPPLEMENTARY NOTES		
19. KEY WORDS (Continue on reverse side if necessary and identify by block number) Heat Transfer; Thermal Insulation; Heat Stress; Protective Clothing; Cold-Weather Clothing; Submarine-Deck-Exposure Suit; Crash-Crew Firefighters' Clothing		
20. ABSTRACT (Continue on reverse side if necessary and identify by block number) The Navy Clothing and Textile Research Facility (NCTRF) studied heat transfer mechanisms in Navy clothing materials to determine their individual effects on total insulation values. The evaluated clothing were the A-1 (or extreme-)cold-weather clothing, the submarine-deck-exposure suit, and the crash-crew firefighters' clothing ensemble. (U)		

(continued)

UNCLASSIFIED

SECURITY CLASSIFICATION OF THIS PAGE(When Data Entered)

This study showed that the only significant heat transfer mechanisms acting in the tested materials were gaseous and solid thermal conduction. The mechanisms of convection and radiational heat transfer were either non-existent or insignificant. Conduction heat transfer models, which were developed to study the contribution of gaseous and solid thermal conduction, permitted good predictability of the measured values for the thermal insulation components of the studied assemblies. These models provided us with a reliable means of estimating insulation values of similar materials. (U)

It was also shown that the quality of the thermal insulation materials in the studied assemblies was very good. The thermal insulation values were slightly less or greater than what can be considered practical maximums for air-filled insulations (1.85 Clo/cm). (U)

To extend our ability to estimate thermal insulation values of materials normally used in Navy protective clothing (fibrous batts and closed cell foams), NCTRF will conduct further studies on these types of materials, which will encompass a broader range of properties than exists in currently used materials. (U)

UNCLASSIFIED

SECURITY CLASSIFICATION OF THIS PAGE(When Data Entered)

TABLE OF CONTENTS

	<u>Page</u>
List of Illustrations	iv
List of Tables	v
Introduction	1
Material Description	2
Procedures	5
Thermal Insulation Tests	5
Thickness Measurements	5
Other Measurements	5
Results	7
Convective Heat Transfer	7
Thermal Radiation	8
Gaseous and Solid Thermal Conduction	9
PVC Foam Materials	10
Aramid Batt	12
Quality of Insulation	15
Discussion of Results	16
Conclusions	17
Future Work	18
Appendix A. Tables.	A-1

Accession For	
NTIS CRA&I	<input checked="" type="checkbox"/>
DTIC TAB	<input type="checkbox"/>
Unannounced	<input type="checkbox"/>
Justification	
By	
Distribution /	
Availability Codes	
Dist	Avail and/or Special
A-1	

LIST OF ILLUSTRATIONS

<u>Figure</u>		<u>Page</u>
1	Thermal Model for PVC Closed-Cell Foam.	11
2	Thermal Models for Aramid Batt.	13

LIST OF TABLES

<u>Table</u>		<u>Page</u>
I	Material Codes	A-2
II	Thermal Insulation Results for Evaluated Assemblies	A-3
III	Percentage of Total Insulation Provided by Component Assemblies	A-6
IV	Physical Characteristics of PVC Foam and Aramid Batt Materials	A-8
V	Effect of Thermal Conductivity and Density Values of Solid PVC on Structural Parameters α and ϵ_p for Closed-Cell Foam Model	A-9
VI	Computed Values for ϵ_p and α for Evaluated PVC Closed-Cell Foam Materials	A-10
VII	Comparison of Porosities Obtained with Parallel and Series Thermal Model Equations and Measured Values	A-11

HEAT TRANSFER MECHANISMS IN NAVY CLOTHING MATERIALS

INTRODUCTION

As part of the Navy Clothing and Textile Research Facility (NCTRF) program to study heat transfer mechanisms in Navy clothing materials, this report contains data on the thermal insulation characteristics of the A-1 (or extreme-)cold-weather clothing, the submarine-deck-exposure suit, and the crash-crew firefighter's ensemble.

The three clothing assemblies were believed to be most representative of the thermal protection methods now used in the design of Navy clothing. The A-1 cold-weather clothing and the submarine-deck-exposure suit represent designs which use the material that protect against wind and rain and have thermal insulation materials that provide inherent buoyancy to the ensemble. The crash-crew firefighters' ensemble contains materials that protect against high-intensity thermal radiation and water and steam penetration. The thermal insulation materials selected for the firefighters' garment are nonflammable and have good resistance to compression.

This report presents thermal insulation test results for the clothing ensembles studied, and it discusses the significant heat transfer mechanisms functioning in these materials and the quality of insulation provided by these assemblies.

MATERIAL DESCRIPTION

The following lists the descriptions of the material assemblies evaluated. The order is from the outer shell material to the material located closest to the body.

1. Extreme-Cold-Weather Impermeable Jacket Mil-J-82299

a. Assembly 1 - Arm Areas

(1) Neoprene-Coated Nylon Twill, Type I - MIL-C-19759, Cloth, Coated, Twill, Nylon (Low Count).

(2) Nylon Taffeta - MIL-C-21852, Cloth, Nylon Taffeta (2.0 oz/yd²).

(3) PVC Closed-Cell Foam - 3.97 mm thick - Type II, Class 6, MIL-P-12420, Plastic Material, Cellular, Elastomeric.

(4) Nylon Taffeta - Same as a. (2) above.

b. Assembly 2 - Torso

(1) Neoprene-Coated Nylon Twill - Same as a. (1).

(2) Nylon Taffeta - Same as a. (2).

(3) PVC Closed-Cell Foam - Same as a. (3).

(4) Nylon Taffeta - Same as a. (2).

(5) Nylon Taffeta - Same as a. (2).

(6) PVC Closed-Cell Foam - Same as a. (3).

(7) Nylon Taffeta - Same as a. (2).

2. Submarine-Deck-Exposure Coveralls - MIL-C-29109

a. Assembly 1 - Arms, Legs, and Lower Torso

(1) Neoprene-Coated Nylon - Same as 1. a. (1).

(2) PVC Closed-Cell Foam
3.2 mm thick - Same as 1. a. (3)

(3) Nylon Taffeta - Same as 1. a. (2).

b. Assembly - Upper Torso Area

- (1) Neoprene-Coated Nylon Twill - Same as 1. a. (1).
- (2) PVC Closed-Cell Foam
6.4 mm thick - Same as 1. a. (3).
- (3) Nylon Taffeta - Same as 1. a. (2).

3. Firemen's Aluminized Proximity Clothing - MIL-T-29146 for Trousers

a. Aluminized Novatex (asbestos/aramid) - MIL-C-29143, Cloth, Coated, Asbestos/Aramid, Plain Weave, Aluminized

b. Neoprene Coated Nylon Taffeta, Type II - MIL-C-19699, Cloth, Coated, Nylon Taffeta

c. Aramid Quilted Batting, Type I - MIL-B-87002, Batting, Quilted, Aramid, 271 g/m². Batting materials were:

(1) Polyamide Twill, Type I - MIL-C-81280, Cloth Twill, Polyamide Aromatic Staple, High-Temperature-Resistant.

(2) Aramid Fiber Needled Batt.

(3) Rayon Satin - Class 1 - MIL-C-368, Cloth, Satin, Rayon and Cloth, Twill Rayon.

The materials used in the various assemblies were coded as shown in Table I. The materials used in the extreme-cold-weather clothing and in the submarine-deck-exposure coveralls were similar. For these clothing assemblies the neoprene-coated nylon-twill material differed only in color, the nylon taffeta was identical, and the PVC foam differed only in thickness. Therefore, the same material codes are used for the various materials in these two clothing ensembles. The functions of the various assembly materials follow.

1. Extreme-Cold-Weather Impermeable Jacket

- a. Neoprene-Coated Nylon Twill - water-proof and wind-proof barrier.
- b. PVC Closed-Cell Foam - thermal insulation and buoyancy.
- c. Nylon Taffeta - containment materials for PVC closed-cell foam.

2. Submarine-Deck-Exposure Coveralls

- a. Neoprene-Coated Nylon Twill - water-proof and wind-proof barrier.
- b. PVC Closed-Cell Foam - thermal insulation and buoyancy.
- c. Nylon Taffeta - inner lining material.

3. Firemen's Aluminized Proximity Clothing

- a. Aluminized Novatex - protection against high-temperature thermal radiation.
- b. Neoprene-Coated Nylon Taffeta - water and steam barrier.
- c. Aramid Batting - thermal insulation.

PROCEDURES

Thermal Insulation Tests

All thermal insulation tests were conducted in a Dynatec Corporation Rapid "K" thermal conductivity apparatus whose design conforms to requirements of ASTM Method C518-70, Thermal Conductivity of Materials by Means of the Heat Flow Meter. The apparatus was calibrated before and after testing with a glass fiberboard standard reference material. The apparatus has a claimed accuracy of $\pm 5\%$. A Leeds and Northrup Trendscan 1000 Datalogger Recorder was used for data acquisition. Data measurements were made after the test sample was in thermal equilibrium. In addition to testing the complete clothing assemblies, we also tested material subassemblies and individual materials. All material configurations were evaluated at two thicknesses determined at pressures of 0.01 and 0.05 psi. The average test temperatures for the materials ranged between 24 and 27°C.

To establish if heat transfer mechanisms other than gaseous or solid conduction were significant, we did the following:

1. All assemblies, subassemblies, and individual materials were tested with the heat flow directed both vertically upward and downward through them. If there were significant differences in computed insulation values because of heat flow orientation, convective heat transfer would be present.
2. The effect of radiation heat transfer was determined on the firefighters' clothing assembly only. The assembly was modified so that each boundary material consisted of the highly reflective aluminized Novatex material utilized in this clothing. This assembly was evaluated with these reflective boundary materials facing outward in direct contact with the hot and cold plates of the apparatus and facing inward toward the clothing assembly. If significant differences in computed insulation values occurred because of the orientation of the aluminized materials, heat transfer by radiation would be present.

Thickness Measurements

The thickness of all material assemblies, subassemblies, and individual materials were measured on a Model TTD Instron Testing Machine over a 130 sq. cm. surface area at pressures of .01 and .05 psi. The pressure loads were held for 5 minutes before thickness readings were taken.

Other Measurements

To further classify the materials studies, we determined material weights on a balance accurate to .01 gram. Using a microscope with a 3-power magnification, we determined the fiber parameters and the pore sizes for the

fibrous and the foam materials, respectively, which were used for thermal insulation in the tested assemblies. The microscope was equipped with a calibrated micronmeter positioner, which was used to measure the fiber diameter and the pore sizes. For the aramid batt materials used in the fire-fighters' clothing, the air permeability was determined with a Frazier Air Permeability Test Apparatus in conformance with Method 5451, Permeability of Cloth, Calibrated Orifice Method, Federal Standard 191.

RESULTS

The thermal insulation results obtained for the various material assemblies and subassemblies are given in Table II. Along with the thermal insulation results, Table II lists pressure, thickness, heat flow orientation, and average sample temperature information in relation to thermal insulation. Table III shows the percentage contributed by subassemblies and the individual materials to the total insulation value for the various assemblies studied. These data will be discussed with respect to the various potential heat flow transmission mechanisms that may have contributed to the measured insulation values--convective heat transfer, thermal radiation, gaseous and solid thermal conduction, and the quality of the insulation.

Convective Heat Transfer

Any influences of gaseous convective heat transfer effects on the insulation data would be shown by differences in insulation results with changes in heat flow direction. It would normally be expected that, if any significant convective effects existed in the untested material assemblies, those results with downward heat flow should show higher thermal insulation results than similar tests with upward heat flow. For example, for laminar airflow across a square horizontal hot surface, the convective heat transfer coefficient when the heat flow is upward is twice as high as for a similar surface facing downward (1)--doubling the heat loss due to convection with heat flow upward (lower effective insulation value).

Hot Plate Facing Up

$$H_c = .54 \frac{k}{L} (Gr_L Pr)^{1/4} \quad \underline{1}$$

Hot Plate Facing Down

$$H_c = .27 \frac{k}{L} (Gr_L Pr)^{1/4} \quad \underline{2}$$

when

H_c = convective coefficient
 k = thermal conductivity of gaseous media
 L = length of a side of the square plate
 Gr_L = Grashof number
 Pr = Prandtl number

Contrary to expectations Table II data show in most cases a lower insulation value when heat flow orientation is downward compared with heat flow upward. These differences are small and are well within the $\pm 5\%$ accuracy range of the measuring device when the average value of any two

(1) Kreith, F., Principles of Heat Transfer, Second Edition, International Textbook Co., 1966, p. 340.

similar results are compared with the individual values. In addition the average sample temperature for those tests where heat flow was upward was about 2°C lower than sample temperatures for heat flow downward. It is well known that a reduction in sample test temperature will contribute to a higher thermal insulation value. The average difference between test results of heat transfer upward and the downward data was approximately 0.03 Clo. Tests of three of the material subassemblies at two different sample temperatures with downward heat flow showed insulation increases of 0.02 to 0.04 Clo for sample temperature reductions of approximately 4.5°C (Table II), indicating that approximately 50% of the differences in insulation values measured for changes in heat flow orientation could be attributable to temperature effects.

The differences in insulation values measured for the two heat flow orientations were very small. Moreover, 50% of these small differences could be associated with differences in sample temperatures. It can be concluded, therefore, that convective heat transfer had no significant influence on the insulation values of the evaluated materials.

Thermal Radiation

The influence of thermal radiation on the effective insulation value was studied only on the crash-crew firefighters' clothing assembly. The fibrous insulation material used in this assembly was permeable (Table IV), as opposed to the impermeable foam used in the other assemblies. Thus, it was felt that, if heat transfer by thermal radiation existed in any of these materials to any significant extent, it would be most noticeable in the permeable fibrous insulation. Heat transfer by thermal radiation can be estimated for a fibrous insulation material from reference (2) as:

$$q_r = \frac{\sigma_s (T_o^4 - T_n^4)}{(n-1) \left[\frac{2}{\epsilon} - 1 + \frac{1}{n-1} \left(\frac{2}{\epsilon_o} - 1 \right) \right]} \quad \underline{3}$$

when

q_r = heat flux due to thermal radiation
 σ_s = Stefan-Boltzmann constant
 T_o = absolute temperature of hot plate
 T_n = absolute temperature of cold plate
 n = number of fibrous layers
 ϵ = emissivity of boundary materials
 ϵ_o = emissivity of fibrous layers

(2) Bankvall, C. G., Heat Transfer in Fibrous Materials, National Swedish Building Research Summaries, D4, 1972.

Assuming $\epsilon\sigma$ is approximately equal to 1 and d is the thickness of the material and L_o the distance between fiber layers, then $n - 1 = d/L_o$. Since d is much greater than L_o (more than 10,000 times greater--compare the fiber diameter of aramid batt with its material thickness data in Table IV), equation 3 can be simplified to:

$$q_r = \frac{\sigma_s L_o}{d} \left(\frac{T_o^4 - T_n^4}{\frac{2}{\epsilon} - 1} \right) \quad \underline{4}$$

for $\epsilon=1$ (Black Boundary Materials)

$$q_r = \frac{\sigma_s L_o}{d} (T_o^4 - T_n^4) \quad \underline{5}$$

For $\epsilon = 0$ (Reflective Boundary Materials)

$$q_r = 0 \quad \underline{6}$$

To effect the above conditions, emissivity characteristics of the hot and cold plates of the apparatus employed in these evaluations were changed to an emissivity approaching 1 and to an emissivity approaching 0 by having the modified firefighter assembly outer reflective materials facing and directly in contact with the hot and cold plates in one case and facing inward to the assembly in the other orientation.

As can be seen from Table II, the insulation results for either orientation of the outer materials were essentially identical, indicating that there was no significant heat transfer through these materials by radiation. Thus, it was concluded that thermal radiation transfer plays no significant role as a heat transfer mechanism in any of the evaluated materials.

Gaseous and Solid Thermal Conduction

From the previous discussions it was established that convective and radiation heat transfer through the materials was either nonexistent or insignificant. The insulation values measured must then have been caused by the effects of gaseous and solid thermal conduction heat transfer through these materials.

Table III shows that only the thermal insulation materials used in the tested assemblies contributed substantially to the overall insulation values. Typically 80% and 95% of the insulation values measured in a complete assembly were related to either the aramid batt in the case of the crash-crew firefighters' ensemble or the PVC foam materials in the extreme-cold-weather jacket and the submarine-deck-exposure coveralls, respectively. The contribution of the outer shell, lining, and interlining materials and the air gaps associated with these layers provided little additional insulation, except for the outer shell material for the firefighters' clothing.

The value for the firefighters' outer shell material was somewhat misleading. The firefighters' outer shell material contributed 17.5% to the total insulation of the assembly at a thickness value associated with a pressure of .01 psi but dropped to 12.6% when the pressure was increased to .05 psi. This shell material is quite stiff. Because there was a sizeable reduction in insulation value when thickness was reduced by increasing the contact pressure, it appears that the contact between the test apparatus plates and the shell material was not uniform at the lower test pressure. This poor contact probably produced an air gap between the outer shell material and the plates. In any event, because the aramid batt and PVC foam materials contributed most of the insulation values measured in the assemblies, NCTRF felt only these materials needed to be studied to determine the contributions of gaseous and solid heat conductive effects.

PVC Foam Materials. Figure 1 shows the thermal model employed to determine the contributions of gaseous and solid conduction in the foam materials. Shown is a unit cube of the structure indicating that heat flow through the structure is initially in tandem through a gas and solid phase and then through the solid phase alone. This model is consistent with the general geometry of a closed-cell foam (gaseous voids surrounded by solid material). The equation relating the apparent thermal conductivity of such a structure to the individual conductivities of the gaseous and solid media is as follows:

$$\lambda_a = \frac{\lambda_s [\lambda_g \alpha + \lambda_s (1 - \alpha)]}{\lambda_s \epsilon p + (1 - \epsilon p) [\lambda_g \alpha + \lambda_s (1 - \epsilon)]} \quad 7$$

When

λ_a = apparent thermal conductivity of the composite material

λ_g = thermal conductivity of gaseous media

λ_s = thermal conductivity of solid material

α and ϵp are structural parameters of the model and are related to the total porosity " ϵ " of the structure as shown in equation 8.

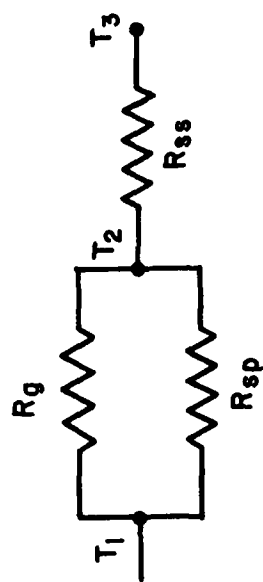
$$\epsilon = \alpha \epsilon p = 1 - \frac{\rho_m}{\rho_s} \quad 8$$

when

ρ_m = density of composite material

ρ_s = density of solid material

If the values of λ_s , λ_g , and ρ_s are known and since λ_a and ρ_m were measured, the structural parameters of the PVC foam (α , ϵp) can be calculated from equations 7 and 8. These values can be used in future applications to predict the apparent conductivities of other similar closed-cell foams. However, literature values for λ_s and ρ_s ranged from .147 to .209 watt/M/°C and from 1.18 to 1.65 g/cc, respectively (Table IV). Consequently, this range of values had to be explored to determine the degree of influence it had on the range of values obtained for the structural parameters (Table V).



R_g - THERMAL INSULATION RESISTANCE OF GAS
IN PARALLEL WITH SOLID PHASE

R_{sp} - THERMAL INSULATION RESISTANCE OF SOLID
IN PARALLEL WITH GAS PHASE

R_{ss} - THERMAL INSULATION RESISTANCE OF SOLID
IN SERIES WITH R_g AND R_{sp}

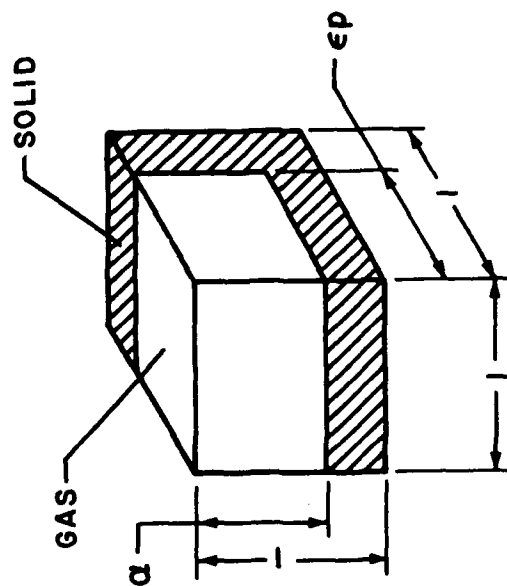


FIGURE I. THERMAL MODEL FOR PVC CLOSED-CELL FOAM.

The range of ϵp and α values computed for all values of λ_s and ρ_s differed from their minimum and maximum values by only 5% or less. Nevertheless, the values in which λ_s was maximum and ρ_s minimum, with respect to the range of values reported for λ_s and ρ_s (Table V), were the only ones for λ_s and ρ_s that produced structural parameter values consistent with the physical model in which both α and ϵp must be less than 1. Since the differences in structural parameter values obtained over the range of λ_s and ρ_s values were small, those values of λ_s and ρ_s that produced ϵp and α values consistent with the physical model were judged as most representative and used in further computations. These values were: $\lambda_s = .209$ watt/M/°C; and $\rho_s = 1.19$ g/cc.

Table VI shows the computed ϵp and α values for six PVC foam materials of approximately the same density and three thickness ranges and approximately the same pore size. These values did not differ appreciably. The average values of ϵp and α were .9937 and .9565, respectively. Although sample thicknesses differed by a ratio as large as 2.4:1, the similarity in the structural parameter values ϵp and α calculated from equations 7 and 9 reaffirms previous statements that heat transfer through these materials was governed primarily by thermal conduction effects. The similarity between ϵp and α values (standard deviation less than $\pm .004$) also indicates that, by use of the structural and thermal characteristics shown in Table VI with equation 7, the prediction of apparent thermal conductivity values of PVC foam having similar properties to those evaluated should be quite accurate.

By comparing the thermal conductivity for the composite material to that of an equivalent solid material (Table VI), we can estimate that the gas cells within the composite PVC material accounts for approximately 84% of the insulation value achieved with the composite. Thus, solid conduction effects account for only 16% of the heat transfer through the composite.

Aramid Batt. Figure 2 shows the thermal models used to represent the aramid batt material to determine how the gaseous and solid components of the composite material contribute to the apparent thermal conductivity of the composite. The parallel-series model shown had been previously established by Bankvall (2) in characterizing thermal conduction heat transfer in glass fiberboard insulation. This model assumes that heat transfer through the composite can be represented by a continuous gas and solid path and a solid-gas series path with all three paths being parallel to each other. This model represents all possible heat flow paths through a material such as the aramid batt. The relationship between the apparent thermal conductivity measured for a material of this type and the individual conductivities of the material components and the structural parameters for this model was given by Bankvall as:

$$\lambda_a = \alpha [\epsilon p \lambda_g + (1 - \epsilon p) \lambda_s] + \frac{(1 - \alpha) \lambda_s \lambda_g}{\lambda_g (1 - \epsilon s) + \lambda_s \epsilon s} \quad 9$$

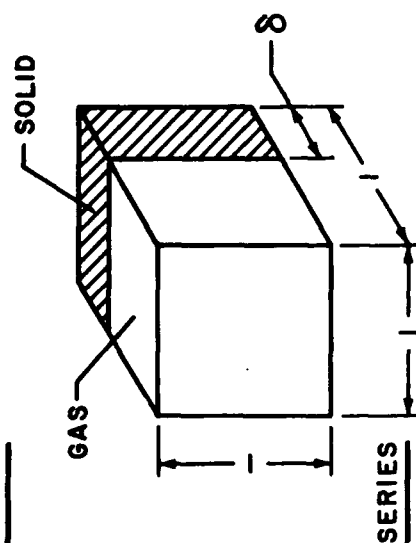
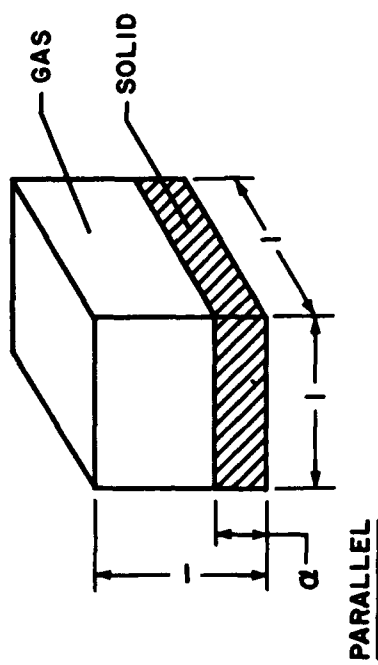
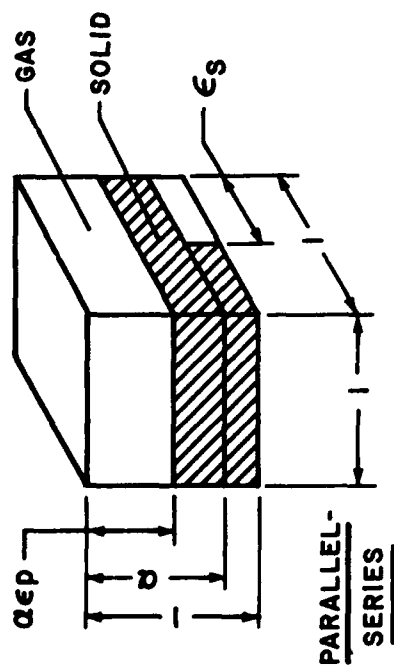
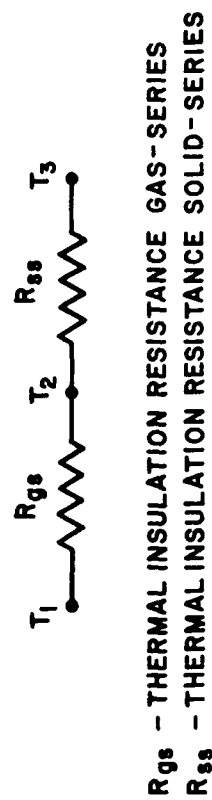
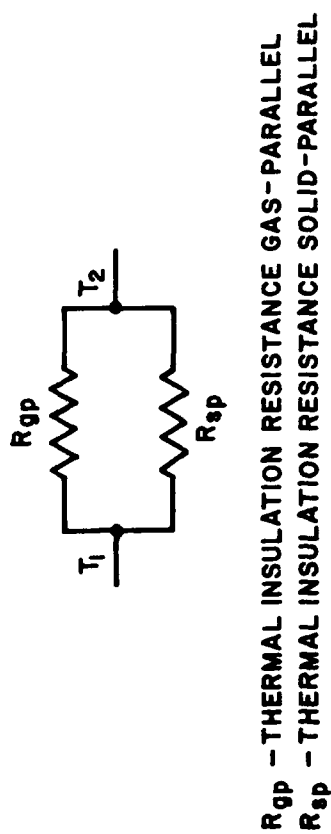
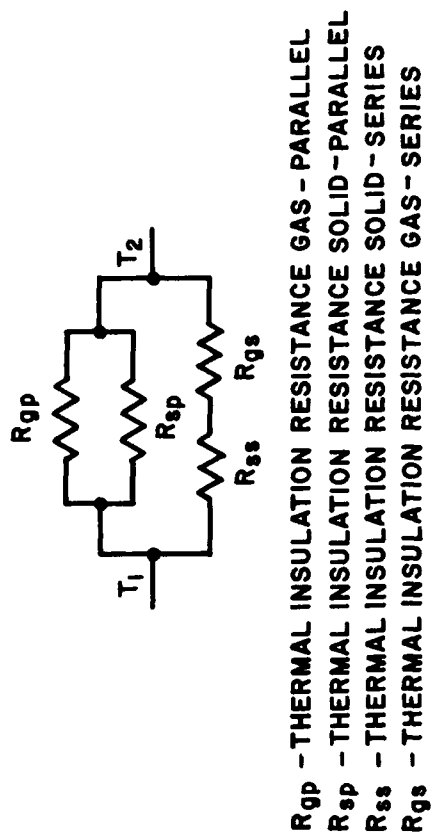


FIGURE 2. THERMAL MODELS FOR ARAMID BATT.

when

α , ϵ_p , and ϵ_s are structural parameters that are related to the total porosity (ϵ) of the material as follows:

$$\epsilon = (1 - \alpha) \epsilon_s + \alpha \epsilon_p \quad 10$$

Because there are three unknowns (α , ϵ_p , and ϵ_s) and only two equations (9 and 10), these structural parameters can be evaluated completely only if thermal insulation tests are conducted under hard vacuum conditions ($\lambda_g = 0$) and under different gas pressures in a range in which λ_g values are affected by pressure differences. Certain factors can thereby be isolated and additional equations developed. Because we did not have this capability, we had to discard this model though we considered it most representative of the heat transfer in the actual material. Instead the data obtained on the aramid batt materials were studied by the use of two simpler thermal models: the pure parallel case of a continuous gas and solid path in parallel and the pure series case of a gas and solid layer in series (Figure 2). Each of these models contains only one structural parameter. The equations governing the thermal conductivity relationship for these models are:

Parallel Case

$$\lambda_a = \lambda_g \left[1 - \alpha \left(1 - \frac{\lambda_s}{\lambda_g} \right) \right] \quad 11$$

Series Case

$$\lambda_a = \lambda_g \left[\frac{1}{1 - \delta \left(1 - \frac{\lambda_g}{\lambda_s} \right)} \right] \quad 12$$

where α and δ are the structural parameters for the parallel and series cases, respectively. The porosity (ϵ) for each case is:

Parallel Case

$$\epsilon = (1 - \alpha) \quad 13$$

Series Case

$$\epsilon = (1 - \delta) \quad 14$$

Table VII shows a comparison of porosities computed by use of the equations governing the parallel and series models with the porosities computed from known material-density information. These data show that, for the parallel model case, the porosities agreed within 3% with the values computed from measured density information. The comparisons between the series model and actual values were relatively poor--differences were as great as 28%. Thus, for the aramid batt materials, the parallel model best represents the contributions of the gas and solid media thermal conductivities to the apparent thermal conductivity of the composite material.

Normally one would expect the series model to predict the heat transfer performance of a batting best, because the material is produced by stacking individual layers together. However, the aramid batt construction is such that it was needed to hold the layers together mechanically. Apparently the increase in fiber-to-fiber conduction caused by needling was such that this mode of heat transfer became dominant with respect to gas to solid transfer. The closeness to which the parallel model predicts the thermal performance of the aramid batt material indicates that good estimates of the thermal conductivity of similar materials can be made using equations 11 and 13. This close agreement also reaffirms that gaseous conduction and solid conduction are the only significant heat transfer mechanisms active in these materials, because the results are almost totally predictable by use of conduction heat transfer relationships.

A comparison of the thermal conductivity values of the aramid batt composite and an equivalent solid material indicates that approximately 86% of the thermal insulation provided by the aramid batt results from the contained gas. Consequently, the solid phase of the composite contributes only 14% to the thermal insulation value. These results were similar to those obtained with the PVC foams.

Quality of Insulation

The thermal insulation values for the clothing assemblies indicated the materials provided good insulation performance. Theoretically, the maximum possible specific insulation value would be obtained with still air with no radiation heat transfer. The value is reported to be 2.56 Clo/cm ($\lambda_a = .0252 \text{ watt/M/}^\circ\text{C}$); however, the practical maximum value for air in narrow horizontal spaces is 1.85 Clo/cm (3). The PVC foam and aramid batt thermal insulation materials used in the evaluated clothing showed average insulation values of 1.91 Clo/cm and 1.81 Clo/cm, respectively. Thus, because horizontal insulation values are above or near the practical maximum for narrow air layers, these insulation systems could not easily be substantially improved.

(3) Lyman, F. and Hollies, N., Clothing, Comfort and Function, Marcel Dekker, Inc., New York, 1970, p. 38.

DISCUSSION OF RESULTS

A study of the various heat transfer mechanisms that might be functioning in the extreme-cold-weather clothing, submarine-deck-exposure coverall, and the firefighters' clothing indicated that only conduction heat transfer effects were significant. Consideration of convective and radiation heat transfer in these clothing assemblies indicated these modes were insignificant or nonexistent.

The aramid batt and PVC foam materials contributed 80 and 95%, respectively, of the thermal insulation provided by the clothing assemblies. Consistent results were obtained by computing the structural parameters for the foam and batt insulation materials. These parameters were derived from the thermal insulation results measured and from applicable thermal heat conduction models and their governing equations. These equations related the gas and solid phase to the apparent thermal conductivity of these materials. The standard deviation for the computed parameters was no more than $\pm .004$. The small differences were further indications that convective and radiation heat transfer modes were not significant in these materials.

Knowing the structural parameters for these materials makes it possible to predict the thermal insulation performance of other similar materials by applying the heat conduction equations 7 or 11, depending upon whether the insulation is a foam or a fibrous batt. The quality of the insulation was high for the clothing assemblies studied. The PVC foam and aramid batt materials showed average specific insulation values of 1.91 and 1.81 Clo/cm, respectively (Table II), which are better or close to the value considered practically achievable with small horizontal air spaces (1.85 Clo/cm). This indicates that making significant improvements in these insulations would be difficult.

The highest specific insulation value possible in air-filled insulations at normal pressures and temperatures is 2.56 Clo/cm (3). This value has been approached only with insulation media using fine powders, such as silica aerogel (4), in which the interstitial space between grains is less than the mean free path between the gas molecules in which the gas no longer acts as a continuum. Its basic molecular character becomes predominant (5), and heat transfer through the space does not result primarily from intermolecular collisions but from molecular transport across the space. This results in a marked decrease in the rate of heat transfer or effective thermal conductivity value of the gas (6). Practical improvements in current insulation would be limited to achieving the same degree of insulation provided by current materials while optimizing other properties of these insulations, such as weight, flexibility, and compressibility.

-
- (4) Lange, Handbook of Chemistry, Tenth Edition, McGraw-Hill Book Co., Inc., New York, 1961, p. 881.
 - (5) Rohsenow, W., and Harnett, J., Handbook of Heat Transfer, McGraw-Hill Book Co., Inc., New York, 1973, p. 9-2.
 - (6) Scott, R. B., Cryogenic Engineering, D. Van Nostrand Co., Inc., Princeton, N.J., 1959, p. 144.

CONCLUSIONS

1. The only significant heat transfer mechanism acting in the A-1 cold-weather, submarine-deck-exposure, and firefighters' clothing ensembles is gaseous and solid thermal conduction. Convective and radiation heat transfer did not significantly influence the measured insulation values.

2. The thermal insulation results achieved for the various material assemblies established that 80% and 95% were contributed by the aramid batt and the PVC foam materials, respectively.

3. Thermal conduction models and their governing equations showed that calculated structural parameters for the PVC foam and the aramid batt materials were quite repeatable. For the PVC foam, ϵ_p and α values were $.9937 \pm .004$ and $.9565 \pm .002$, respectively. For the aramid batt material, average ϵ values calculated from the model agreed with average ϵ values calculated from measured values of ρ_m within 2%-- $.956 \pm .001$ and $.938 \pm .005$, respectively.

4. The close agreement between the thermal models developed and the measured thermal insulation results in the PVC foam and the aramid batt materials indicate that predictions of apparent thermal conductivity values of similar materials would be quite reliable.

5. The quality of insulation in the clothing ensembles was high with respect to what could be expected to be a practical maximum--1.81 to 1.91 Clo/cm for the aramid batt and the PVC foam materials versus 1.85 Clo/cm for small horizontal air spaces.

6. Because of the high quality of insulation that exists in the clothing ensembles studied, improvement efforts would be best directed to reducing weight and compressibility and improving flexibility of materials while maintaining current insulation values.

FUTURE WORK

Most Navy protective clothing applications require good thermal insulation performance. The insulation materials normally used are either fibrous batts or closed-cell foams. Predictability of the apparent thermal conductivities of these material classes should be extended over a broader range than was accomplished in this study with currently used materials. Therefore, a number of fibrous-batt and closed-cell-foam materials will be evaluated, which are constructed from different materials, densities, and thicknesses.

When the insulation values of a range of these materials are evaluated at different thicknesses, densities, and mean sample temperatures, the structural parameters of these materials will be determinable and, if consistent, will provide predictable thermal performance means.

APPENDIX A. TABLES

Table I. Material Codes

Code No.	Material
1	Neoprene-Coated Nylon Twill
2	Nylon Taffeta
3	PVC Closed-Cell Foam
4	Aluminized Novatex
5	Neoprene-Coated Nylon Taffeta
6A	Aramid Batting
6B	Aramid Batting

Table II. Thermal Insulation Results for Evaluated Assemblies

Clothing Assembly	Configuration ¹	Press (psi)	Thick (cm)	Heat Flow Direction	Avg. Sample Temp. (°C)	Thermal Insulation	
						Intrinsic (Clo)	Specific (Clo/cm)
Extreme Cold Weather Jacket Assembly-1	1-2-3-2	.01	.452	Down	26.3	.79	1.75
				Up	23.8	.82	1.81
		.05	.429	Down	26.3	.77	1.79
				Up	23.9	.80	1.87
	2-3-2	.01	.422	Down	26.8	.76	1.79
				Up	24.4	.79	1.86
		.05	.404	Down	26.3	.72	1.78
				Up	24.6	.75	1.86
	3	.01	.399	Down	26.5	.75	1.87
				Up	24.3	.77	1.94
Extreme Cold Weather Jacket Assembly-2	1-2-3-2-2-3-2	.01	.859	Down	26.0	1.56	1.81
				Up	24.3	1.56	1.81
		.05	.823	Down	26.3	1.44	1.75
	2-3-2-2-3-2	.01	.828	Down	26.0	1.51	1.83
				Up	24.5	1.54	1.86
		.05	.798	Down	26.2	1.44	1.80
	2-3-2	.01	.396	Down	31.6	.70	1.78
				Down	26.8	.73	1.84
				Up	24.4	.75	1.89
		.05	.376	Down	26.9	.70	1.85
				Up	24.4	.73	1.93
		.01	.422	Down	26.6	.79	1.87
	2-3-2	.01	.422	Down	26.6	.79	1.87
				Up	24.7	.82	1.94
		.05	.401	Down	31.3	.72	1.80
				Down	26.6	.74	1.85
				Up	24.6	.77	1.93

¹ The numbers correspond to the material codes in Table I.

Table II. Thermal Insulation Results for Evaluated Assemblies (cont'd)

Clothing Assembly	Configuration	Press (psi)	Thick (cm)	Heat Flow Direction	Avg Sample Temp. (°C)	Thermal Insulation	
						Intrinsic (Clo)	Specific (Clo/cm)
Sub-marine Deck Exposure Coveralls Assembly-1	1-3-2	.01	.754	Down	26.2	1.39	1.84
				Up	24.1	1.33	1.76
		.05	.737	Down	26.2	1.34	1.82
				Up	24.7	1.35	1.83
	3-2	.01	.721	Down	26.4	1.37	1.89
				Up	24.8	1.35	1.87
		.05	.709	Down	26.2	1.35	1.91
				Up	24.8	1.34	1.88
	3	.01	.711	Down	26.3	1.35	1.91
				Up	24.7	1.38	1.94
		.05	.696	Down	26.9	1.30	1.87
				Up	24.7	1.33	1.91
Sub-marine Deck Exposure Coveralls Assembly-2	1-3-2	.01	.389	Down	26.9	.69	1.78
				Up	24.1	.72	1.86
		.05	.366	Down	26.8	.62	1.69
				Up	24.2	.66	1.79
	3-2	.01	.353	Down	26.7	.64	1.83
				Up	24.0	.67	1.90
		.05	.335	Down	27.1	.60	1.80
				Up	24.1	.64	1.90
	3	.01	.340	Down	26.8	.64	1.90
				Up	23.9	.67	1.98
		.05	.320	Down	26.4	.59	1.84
				Up	23.9	.62	1.94

Table II. Thermal Insulation Results for Evaluated Assemblies (cont'd)

Clothing Assembly	Configuration	Press (psi)	Thick (cm)	Heat Flow Direction	Avg Sample Temp. (°C)	Thermal Insulation	
						Intrinsic (Clo)	Specific (Clo/cm)
Firemen's Aluminized Proximity Clothing	4-5-6A	.01	.796	Down	30.6	1.32	1.66
				Down	26.3	1.36	1.71
				Up	25.3	1.38	1.74
		.05	.671	Down	26.4	1.10	1.63
				Up	25.2	1.12	1.67
	5-6A	.01	.658	Down	26.4	1.16	1.77
				Up	24.8	1.19	1.81
		.05	.569	Down	26.4	1.01	1.78
				Up	25.0	1.04	1.83
Firemen's Aluminized Proximity Clothing Modified	6A	.01	.620	Down	26.3	1.11	1.79
				Up	24.7	1.14	1.84
		.05	.538	Down	26.1	.95	1.77
				Up	24.7	.98	1.82
	6B	.01	.607	Down	26.0	1.09	1.79
				Up	24.3	1.12	1.85
		.05	.523	Down	25.7	.93	1.79
				Up	24.3	.96	1.84
Firemen's Aluminized Proximity Clothing Modified	4-5-6A-4 Aluminum Facing Hot and Cold Plates	.01	.859	Down	25.5	1.38	1.61
				Up	24.5	1.41	1.64
		.05	.732	Down	25.9	1.13	1.54
				Up	24.5	1.16	1.58
	4-5-6A-4 Aluminum Facing in Toward Assembly	.01	.859	Down	26.1	1.38	1.61
				Up	24.8	1.42	1.65
		.05	.732	Down	25.8	1.13	1.54
				Up	24.6	1.16	1.58

Table III. Percentage of Total Insulation Provided by Component Assemblies

Clothing Assembly	Configuration	Thickness (cm)	Avg. Sample Temp. (C°)	Thermal Insulation		Percent of Total Insulation (%)
				Intrinsic (Clo)	Specific (Clo/cm)	
Extreme Cold Weather Jacket Assembly-1	1-2-3-2	.452	25.1	.81	1.79	100
		.429	25.1	.79	1.84	100
	2-3-2	.422	25.6	.78	1.85	96.3
		.404	25.5	.74	1.83	93.7
	3	.399	25.4	.76	1.90	93.8
		.381	25.5	.73	1.92	92.4
	1	.030	25.3	.03	1.00	3.7
		.025	25.3	.05	2.00	6.3
	2	.012	25.5	.01	.83	1.2
		.012	25.5	.005	.42	.6
Extreme Cold Weather Jacket Assembly-2	1-2-3-2-	.859	25.2	1.56	1.82	100
	2-3-2	.823	25.4	1.47	1.79	100
	2-3-2-2-	.828	25.3	1.53	1.85	98.1
	3-2	.798	25.4	1.46	1.83	99.3
	2-3-2	.396	25.6	.74	1.87	47.4
		.376	25.7	.72	1.91	49.0
	2-3-2	.422	25.7	.81	1.92	51.9
		.400	25.6	.76	1.90	51.7
	1	.031	25.3	.03	.97	1.9
		.025	25.4	.01	.40	0.7
Submarine Deck Exposure Coveralls Assembly-1	1-3-2	.754	25.2	1.36	1.80	100
		.737	25.5	1.35	1.83	100
	3-2	.721	25.6	1.36	1.89	100
		.709	25.5	1.35	1.90	100
	3	.711	25.5	1.37	1.93	100
		.696	25.8	1.32	1.90	97.8
	1	.033	25.4	0.0		0.0
		.028	25.5	0.0		0.0
	2	.010	25.6	0.0		0.0
		.013	25.7	0.03	2.30	2.2

Table III. Percentage of Total Insulation Provided by Component Assemblies
(cont'd)

Clothing Assembly	Configuration	Thickness (cm)	Avg. Sample Temp. (C°)	Thermal Insulation		Percent of Total Insulation (%)
				Intrinsic (Clo)	Specific (Clo/cm)	
Submarine Deck Exposure Coveralls Assembly-2	1-3-2	.389	25.5	.71	1.83	100
		.366	25.5	.64	1.75	100
	3-2	.353	25.4	.66	1.87	93.0
		.335	25.6	.62	1.85	96.9
	3	.340	25.4	.66	1.94	93.0
		.320	25.2	.61	1.91	95.3
	1	.049	25.5	.05	1.02	7.0
		.046	25.4	.02	.43	3.1
	2	.031	25.4	.00		0.0
		.015	25.4	.01	.67	1.6
Firemen's Aluminized Proximity Clothing	4-5-6A	.796	25.8	1.37	1.72	100
		.671	25.8	1.11	1.65	100
	5-6A	.658	25.6	1.18	1.79	86.1
		.569	25.7	1.03	1.81	92.8
	6A	.620	25.5	1.13	1.82	82.5
		.538	25.4	.97	1.80	87.4
	4	.138	25.7	.24	1.74	17.5
		.102	25.8	.14	1.37	12.6
	5	.038	25.6	.05	1.32	3.6
		.031	25.6	.06	1.94	5.4

Table IV. Physical Characteristics of PVC Foam and Aramid Batt Materials

Material	Fiber Dia. (microns)	Pore size (mm)	Thick (cm)		Density (g/cc)		Density Solid (g/cc)	Therm. Cond. (Watt/Meter deg C)		Air Permeability (cu ft/sq ft/min)
			.01 psi	.05 psi	.01 psi	.05 psi		Solid ¹	Air ²	
PVC Foam			.340	.320	.0606	.0644	1.18 to 1.65 ¹	.147 to .209	.0257	
		.548±.23	.399	.381	.0556	.0583	1.18 to 1.65 ¹	.147 to .209	.0257	
		.507±.15	.710	.696	.0553	.0565	1.18 to 1.65 ¹	.147 to .209	.0257	
Aramid Batt	27.5		.620	.538	.0810	.0934	1.38 ³	.251	.0257	25.6
	27.5		.607	.523	.0777	.0902	1.38 ³	.251	.0257	27.0

¹ See reference 4.

² See reference 1.

³ Fibers, Organic, Man-Made.

Table V. Effect of Thermal Conductivity and Density Values of Solid PVC on Structural Parameters α and ϵ_p for Closed-Cell Foam Model

Thermal Conductivity (Watt/Meter/Deg C)			Density (g/cc)		Structural Parameters		
λa^1	λg	λs	ρm	ρs	ϵ	ϵp	α
.0336	.0257	.147	.0553	1.180	.9531	1.0255	.9294
		.163	.0553	1.415	.9609	1.0364	.9272
				1.650	.9665	1.0443	.9255
				1.180	.9531	1.0143	.9397
		1.415	.9609	1.0248	.9376		
		1.650	.9665	1.0323	.9363		
		.209	.0553	1.180	.9531	.9953	.9576
				1.415	.9609	1.0050	.9561
				1.650	.9665	1.0119	.9551

¹.0336 watt/meter/deg C (1.91 Clo/cm) average apparent thermal conductivity value measured on PVC foam component of the Extreme-Cold-Weather Jacket, Assembly 1.

Table VI. Computed Values for ϵ_p and α for Evaluated PVC Closed-Cell Foam Materials

Clothing	Thick (cm)	Thermal Conductivity (W/M/Deg C)			Density (g/cc)		Structural Parameters		
		λ_a	λ_g	λ_s	ρ_s	ρ_m	ϵ	ϵ_p	α
Extreme-Cold- Weather Jacket Assembly 1	.399	.0336	.0257	.209	1.18	.0553	.9531	.9953	.9576
	.381	.0342				.0565	.9521	.9981	.9539
Sub-Deck Exposure Suit Assembly 1	.711	.0338	.0257	.209	1.18	.0556	.9529	.9963	.9564
	.696	.0340				.0583	.9506	.9948	.9556
Sub-Deck Exposure Suit Assembly 2	.340	.0333	.0257	.209	1.18	.0606	.9486	.9877	.9604
	.320	.0342				.0644	.9454	.9897	.9552
Average		.0339	.0257	.209	1.18			.9937 +.004	.9565 +.002

Table VII. Comparison of Porosities Obtained with Parallel and Series Thermal Model Equations and Measured Values

Material	Thick (cm)	Thermal (Watt/Meter/deg C)			Density (g/cc)		Porosity (ϵ)		
		λ_a	λ_g	λ_s	ρ_s	ρ_m	Actual	Parallel Model	Series Model
Aramid Batt	.620	.0355	.0257	.251	1.38	.0810	.941	.956	.692
	.538	.0359	.0257	.251	1.38	.0934	.932	.955	.683
	.607	.0355	.0257	.251	1.38	.0777	.944	.956	.692
	.523	.0355	.0257	.251	1.38	.0902	.935	.956	.692
Average							.938 $\pm .005$.956 $\pm .001$.690 $\pm .005$